Infrared and infrared emission spectroscopic study of selected magnesium carbonate minerals: artinite and dypingite

Ray L. Frost • **and Silmarilly Bahfenne**

Inorganic Materials Research Program, School of Physical and Chemical Sciences, Queensland University of Technology, GPO Box 2434, Brisbane Queensland 4001, Australia.

Abstract

The proposal to remove greenhouse gases by pumping liquid carbon dioxide several kilometres below ground level implies that many carbonate containing minerals will be formed. Among these minerals, are dypingite and artinite. This necessitates a study of these minerals.

These two hydrated hydroxy carbonate bearing minerals have been characterised by a combination of infrared and infrared emission spectroscopy. Infrared emission spectroscopy is especially useful for the determination of the stability of these minerals. The infrared spectra of artinite and dypingite are characterised by sharp intense OH and water stretching vibrations. Intense $(CO_3)^{2-}$ symmetric and antisymmetric stretching vibrations support the concept that the carbonate ion is distorted, with consequential reduction in symmetry. The position of the water bending vibration indicates the water is strongly hydrogen bonded in the mineral structure.

Key words: artinite, dypingite, carbonate, infrared, infrared emission spectroscopy, Vibrational spectroscopy

Introduction

Geosequestration is a process which involves pumping liquefied carbon dioxide into geological reservoirs at significant distances below the earth's surface.

• Author to whom correspondence should be addressed (r.frost@qut.edu.au)

The proposal to remove green house gases by pumping liquid CO_2 several kilometres below the ground, implies that many carbonate containing minerals [1] will be formed [2, 3]. The ability to be able to easily and readily detect minerals is of importance [4, 5]. This is especially so where carbonate minerals are concerned. The technique of infrared spectroscopy does meet these requirements. What is not known is that many carbonate containing minerals especially the secondary minerals are at least partially soluble and can translocate. Two magnesium carbonate minerals which may form under such conditions of high CO_2 partial pressure are dypingite $Mg_5(CO_3)_4(OH)_2.5H_2O$ [6-10] and artinite $Mg_2(CO_3)(OH)_2.3H_2O$ [11-20].

Many infrared studies have been applied to minerals and soils [21-29]. Many papers have been published on the infrared spectra of carbonate minerals [11, 25-27, 30-32]. The infrared spectra of dypingite was first published by the discoverer Raade [10]. Many carbonate minerals contain both coordinated water and adsorbed water; several minerals contain hydroxyl groups. Thus in these minerals the symmetry of the carbonate anion is reduced to C_{2h} or even C_s [14, 16-18]. This paper reports the infrared and infrared emission spectroscopy of selected hydrated hydroxy magnesium carbonate minerals: artinite and dypingite.

Experimental

Minerals

The following minerals were used in this research (a) Dypingite - Yoshikawaite, Shinshiro Shi, Aichi Prefecture, Japan (b) Sample 4 Dypingite - Clear Creek District, Southern San Benito County, California (c) Sample 3 Artinite - Clear Creek District, Southern San Benito County, California (d) Sample 7 Artinite - Higasi-Kuroda-Guchi, Inasa-Cho, Inasa-Gun, Aichi Prefecture, Japan. The phase purity of the minerals was checked by X-ray diffraction and the chemical composition by EDX measurements.

IR spectroscopy

Infrared spectra were obtained using a Nicolet Nexus 870 FTIR spectrometer with a smart endurance single bounce diamond ATR cell. Spectra over the 4000–525 cm^{-1} range were obtained by the co-addition of 64 scans with a resolution of 4 cm^{-1} and a mirror velocity of 0.6329 cm/s. Spectra were co-added to improve the signal to noise ratio. These spectra are fundamentally reflectance spectra and are transformed to absorbance type spectra.

Band component analysis was undertaken using the Jandel 'Peakfit' (Erkrath, Germany) software package which enabled the type of fitting function to be selected and allows specific parameters to be fixed or varied accordingly. Band fitting was done using a Lorentz-Gauss cross-product function with the minimum number of component bands used for the fitting process. The Lorentz-Gauss ratio was maintained at values greater than 0.7 and fitting was undertaken until reproducible results were obtained with squared correlations (r^2) greater than 0.995. Band fitting of the spectra is quite reliable providing there is some band separation or changes in the spectral profile.

Infrared emission spectroscopy

FTIR emission spectroscopy was carried out on a Nicolet Nexus 870 FTIR spectrometer, which was modified by replacing the IR source with an emission cell. A description of the cell and principles of the emission experiment have been published elsewhere. Approximately 0.2 mg of the carbonate mineral was spread as a thin layer on a 6 mm diameter platinum surface and held in an inert atmosphere within a nitrogen-purged cell during heating. The infrared emission cell consists of a modified atomic absorption graphite rod furnace, which is driven by a thyristor-controlled AC power supply capable of delivering up to 150 amps at 12 volts. A platinum disk acts as a hot plate to heat the artinite sample and is placed on the graphite rod. An insulated 125-μm type R thermocouple was embedded inside the platinum plate in such a way that the thermocouple junction was <0.2 mm below the surface of the platinum. Temperature control of ± 2°C at the operating temperature of the artinite

sample was achieved by using a Eurotherm Model 808 proportional temperature controller, coupled to the thermocouple.

In the normal course of events, three sets of spectra are obtained: firstly the black body radiation over the temperature range selected at the various temperatures, secondly the platinum plate radiation is obtained at the same temperatures and thirdly the spectra from the platinum plate covered with the sample. Normally only one set of black body and platinum radiation is required. The emittance spectrum at a particular temperature was calculated by subtraction of the single beam spectrum of the platinum backplate from that of the platinum + sample, and the result ratioed to the single beam spectrum of an approximate blackbody (graphite). This spectral manipulation is carried out after all the spectral data has been collected.

The emission spectra were collected at intervals of 50°C over the range 200 - 750 °C. The time between scans (while the temperature was raised to the next hold point) was approximately 100 seconds. It was considered that this was sufficient time for the heating block and the powdered sample to reach temperature equilibrium. The spectra were acquired by coaddition of 64 scans for the whole temperature range (approximate scanning time 45 seconds), with a nominal resolution of 4 cm^{-1}. Good quality spectra can be obtained providing the sample thickness is not too large. If too large a sample is used then the spectra become difficult to interpret because of the presence of combination and overtone bands. Spectral manipulation such as baseline adjustment, smoothing and normalisation was performed using the Spectracalc software package (Galactic Industries Corporation, NH, USA).

Results and discussion

Mid-infrared spectroscopy

The infrared reflectance spectra of dypingite and artinite in the 525 to 1625 cm^{-1} region are shown in Figures 1a and 1b and 2a and 2b respectively. The fundamental infrared data has been published [33]. However in order to understand the infrared emission spectra the figures are re-presented here. The sharp bands at

1071 cm^{-1} (Yoshikawaite) and the shoulder at 1078 cm^{-1} (Clear Creek) are attributed to the CO_3^{2-} carbonate symmetric stretching mode. The observation of this mode in the infrared spectra provides evidence for the distortion of the carbonate anion and consequential loss of symmetry. The symmetry of the carbonate anion is reduced to C_{2v} or even C_s. Such reduction in symmetry has been reported by Edwards et al. [11]. Such a band should be not observed in the infrared spectrum but would be intense in the Raman spectrum. The band is observed at 1076 cm^{-1} for artinite (Clear Creek) and 1083 cm^{-1} for the Aichi artinite. . The CO_3^{2-} symmetric stretching mode is complimented with the antisymmetric stretching modes found in the 1300 to 1450 cm^{-1} region where a series of overlapping bands may be observed providing a complex spectral profile. For the dypingite from Clear Creek, these CO_3^{2-} anti symmetric stretching bands are observed at 1312, 1438, 1534 and 1585 cm^{-1}. These bands appear better defined for the Yoshikawaite dypingite with clearly resolved bands at 1380, 1405, 1479 1509 cm^{-1}. For the artinite minerals these CO_3^{2-} antisymmetric stretching modes are observed at 1325, 1381, 1439 cm^{-1} (Aichi) and 1376, 1441, 1535 cm^{-1} (Clear Creek).

In the spectrum of the Yoshikawaite dypingite two bands are observed at 1599 and 1682 cm^{-1}. The assignment of these two bands is to the water HOH bending mode. The fact that two bands are observed suggests that there are two types of water present in the dypingite mineral. The band at 1599 cm^{-1} is attributed to non-hydrogen bonded water and corresponds to the position of the water bending mode of water as water vapour. This band may be attributed to adsorbed water. Whereas the band at 1682 cm^{-1} corresponds to strongly hydrogen bonded water. For artinite two bands are observed at 1578 and 1643 cm^{-1}. This later band shows that the water is very strongly hydrogen bonded. This band corresponds to the water stretching vibration at 2943 cm^{-1} whereas the 1595 cm^{-1} band is reflected in the OH stretching region by the bands in the 3200 to 3450 cm^{-1} region. The observation of the two bands at 1682 cm^{-1} (dypingite) and 1643 cm^{-1} (artinite) suggests that strongly bonded water is important for the stability of these minerals.

Two intense infrared bands are observed at 948 and 1008 cm^{-1} (Yoshikawaite dypingite) and 947 and 1012 cm^{-1} (Clear Creek). These bands are observed at 947 and 1017 cm^{-1} for the Clear Creek sample and at 952 and 995 cm^{-1} for the Aichi

mineral. One possible assignment of these bands is to the OH deformation modes of the MgOH units. These bands may combine to form overtones of the fundamental OH bands. For the Yoshikawaite dypingite infrared spectrum low intensity infrared bands are observed at 755 and 799 cm^{-1}. For the Aichi artinite these bands are observed at 722 and 762 cm^{-1}. These bands are assigned to the $(CO_3)^{2-}$ ν_4 bending modes. The observation of more than one band supports the concept that there are multiple $(CO_3)^{2-}$ bending modes as a result of the distortion of the $(CO_3)^{2-}$ units in the dypingite and artinite structures. For the Yoshikawaite dypingite infrared spectrum two bands are observed at 852 and 882 cm^{-1}. These bands are assigned to the $(CO_3)^{2-}$ ν_2 bending modes. A very low intensity band is observed for the Clear Creek artinite at 844 cm^{-1} which may correspond with this assignment. Two bands are observed at 548 and 618 cm^{-1} for the Clear Creek dypingite and at 546 and 600 cm^{-1} for the Yoshikawaite dypingite. For the clear Creek artinite the bands are observed at 552 and 610 cm^{-1} and at 568 and 638 cm^{-1} for the Aichi artinite. These bands are too low in position to be interpreted as $(CO_3)^{2-}$ bending modes. One possible assignment of these bands is to the water librational modes.

The infrared reflectance spectra of dypingite and artinite are shown in Figures 3 and 4. The infrared spectra of dypingite in the OH stretching region displays two features: (a) two sharp bands at around 3647 and 3686 cm^{-1} and (b) a number of broad overlapping bands centred upon 3289, 3380, 3447 cm^{-1} (Yoshikawaite). The first two bands are assigned to the hydroxyl stretching vibrations of OH units whereas the broad bands are assigned to water stretching bands. The infrared bands at 2887, 2995, 2921 and 2959 cm^{-1} in Yoshikawaite dypingite is ascribed to overtone and combination bands of the OH bending modes. The presence and identification of these bands confirms the presence of strong hydrogen bonds in the structure of dypingite. The variation in intensity of the water OH stretching bands shows that some variation in the formula of dypingite may occur and is a function of the water partial pressure. This variation in intensity is readily observed in Figure 1. Such variation in intensity of the bands assigned to water stretching vibrations may be complicated by the adsorption of water on the mineral surface. The same explanation is suitable for the mineral artinite. Two sharp bands at 3649 and 3685 cm^{-1} are observed for the Clear creek artinite and three bands at 3651, 3685 and 3696 cm^{-1} for

the Aichi artinite. These bands are attributed to the stretching vibrations of the OH units. The other bands in the spectra are assigned to water stretching bands.

Thin Film Infrared emission spectroscopy

Typical infrared emission spectra of artinite and dypingite over the temperature range ambient to 1000°C are shown in Figures 5 and 6. What is clearly observed is (a) the dehydration of artinite by 200°C (b) the loss of intensity in the OH stretching bands by 600°C (c) the loss of intensity in the $(CO_3)^{2-}$ stretching vibrations by the same temperature. The same observations are concluded from the infrared emission spectra of dypingite.

The infrared emission spectra of artinite at 200, 400 and 600°C in the 635 to 1235 cm^{-1} range are shown in Figure 7. In the 200°C spectrum two bands are observed at 1076 and 1093 cm^{-1} and are assigned to the $(CO_3)^{2-}$ stretching vibration. These bands should be infrared inactive but because of the distortion of the carbonate anion and consequential loss of symmetry the bands become infrared activated. The observation of two symmetric stretching modes provides an indication of two non-equivalent carbonate units in the artinite structure. In the 400°C IE spectrum the two bands appear to overlap to form a broad band centred upon 1073 cm^{-1}. In the 600°C spectrum the intensity of this band(s) approaches zero. The two bands in the 200°C spectrum at 946 and 1016 cm^{-1} are attributed to the MgOH deformation modes. The observation of more than one band provides evidence for the non-equivalence of the OH units in the artinite structure. The bands are observed at 940 and 1003 cm-1 in the 400°C spectrum and form a very broad band centred upon 997 cm^{-1} in the 600°C spectrum. The quite intense band at 869 cm^{-1} is assigned to the $(CO_3)^{2-}$ ν_2 bending vibration. Two bands are found in the 400°C spectrum at 839 and 852 cm^{-1} which appear to overlap with a band at 853 cm^{-1} in the 600°C spectrum. The observation of two bands in the 400°C spectrum suggests that the distortion of the carbonate anion is retained as the artinite is heated.

A somewhat similar description applies to the IE spectra of dypingite at 200, 400 and 600°C (Figure 8). The band at 1076 cm^{-1} in the 200°C spectrum; 1073 cm^{-1} (400°C and 1065 cm^{-1} (600°C) is assigned to the $(CO_3)^{2-}$ ν_1 symmetric stretching vibration. Compared with the spectrum for artinite, only a single band is observed even though the band is broad. The infrared bands at 973 and 1015 cm^{-1} in the 200°C spectrum are ascribed to the MgOH deformation bands. These bands broaden with temperature increase and a broad band is observed at 962 cm^{-1} in the 600°C spectrum. The two bands at 853 and 877 cm^{-1} in the 200°C spectrum are assigned to the $(CO_3)^{2-}$ ν_2 bending vibration. These two bands are observed at 844 and 858 cm^{-1} in the 400°C spectrum and broaden in the 600°C spectrum.

The infrared spectra of artinite and dypingite at 200, 400 and 600°C are shown in Figures 9 and 10. This region is where the $(CO_3)^{2-}$ ν_3 antisymmetric stretching vibrations are found. In the 200°C spectrum of artinite multiple bands are observed at 1312, 1317, 1441, 1564 cm^{-1} and in the 400°C spectrum two bands are observed at 1415 and 1549 cm^{-1}. The intensity of these bands diminished in the 600°C spectrum where two bands are found at 1499 and 1575 cm^{-1}. A similar set of bands is provided for the infrared spectrum of dypingite (Figure 10). For the 200°C spectrum bands are observed at 1379, 1417, 1487, 1455 and 1544 cm^{-1} and are attributed to the $(CO_3)^{2-}$ ν_3 antisymmetric stretching vibrations. In the 400°C the number of bands is reduced and in the 600 °C spectrum only remnant intensity remains. Based upon the intensity of bands in this spectral region for dypingite, the thermal stability of dypingite is less than that of artinite.

The infrared spectra of artinite and dypingite at 200, 400 and 600°C are shown in Figures 11 and 12. In the 200°C spectrum of artinite, bands are observed at 3577, 3609, 3653 and 3685 cm^{-1} and are attributed to the OH stretching vibrations of the MgOH units. The bands below 3435 cm^{-1} are assigned to water stretching vibrations. In the 400°C spectrum of artinite, bands are observed at 3645, 3681 and 3727 cm^{-1} and in the 600°C spectrum of artinite, bands are observed at 3644, 3676 and 3721 cm^{-1}. The bands at 2654 and 3586 cm^{-1} are assigned to water stretching vibrations. The intensity of these bands approaches zero in the 600°C spectrum.

For dypingite, in the 200°C spectrum infrared bands are observed at 3618, 3650 and 3685 cm^{-1} and are assigned to the MgOH stretching vibrations. The band at 3516 cm^{-1} is ascribed to water stretching bands. The intensity of this band diminishes in the 400 and 600°C spectrum. The MgOH stretching vibrations are found at 3645, 3681 and 3727 cm^{-1} in the 400°C spectrum and 3644, 3676 and 3721 cm^{-1} in the 600°C spectrum. Significant intensity remains in these bands at this temperature implying that the dehydroxylation of artinite occurs at a higher temperature. For dypingite, infrared bands are observed at 3618, 3650 and 3685 cm^{-1} and are assigned to MgOH stretching vibrations. The band at 3516 cm^{-1} is ascribed to water stretching vibrations. In the 400°C spectrum of dypingite, two bands are displayed at 3650 and 3681 cm^{-1}; in the 600°C spectrum, two overlapping bands are found at 3637 and 3668 cm^{-1}.

Conclusions

There is a need to understand the chemistry of formation of carbonate minerals and their thermal stability. Such formation of the carbonates of magnesium and calcium are essential for the geosequestration of greenhouse gases. The concept of geosequestration involves the pumping of green house gases to significant depths below the surface of the earth. The high partial pressure of liquid CO_2 is significant in that many different types of carbonates will be formed. Among these minerals there is the possibility of the formation of dypingite and artinite which are formed at reasonably low temperatures. Such minerals are readily identified by infrared reflectance spectroscopy. The two minerals dypingite and artinite are closely related and the artinite may transform through thermal treatment to dypingite [10, 15]. Thus the infrared spectra of the two minerals should show a strong resemblance.

A combination of infrared and infrared emission spectroscopy has been used to characterise the two minerals artinite and dypingite and the bands related to the mineral structure. Infrared emission spectroscopy is a powerful technique for the determination of the stability of these hydrated hydroxyl carbonates. The technique can determine the changes in the molecular structure of for example artinite and dypingite as the mineral is decomposed.

Two sharp bands for artinite are observed at 3647 and 3686 cm^{-1} are assigned to the stretching vibrations of the MgOH units and a number of broad overlapping bands centred upon 3289, 3380, 3447 cm^{-1} are assigned to water stretching bands. Multiple bands at 3577, 3609, 3653 and 3685 cm^{-1} are attributed to the OH stretching vibrations of the MgOH units. Intensity of these bands is lost by 600°C. Two bands for artinite observed at 1076 and 1093 cm^{-1} in the 200°C spectrum are assigned to the $(CO_3)^{2-}$ ν_1 stretching vibrations, suggesting the non-equivalence of the carbonate units in the artinite structure. In comparison only as single band at 1076 cm^{-1} is observed for dypingite. In the 200°C spectrum of artinite multiple bands are observed at 1312, 1317, 1441, 1564 cm^{-1} supporting the reduction of symmetry as the artinite is thermally treated.

Acknowledgments

The financial and infra-structure support of the Queensland University of Technology, Inorganic Materials Research Program is gratefully acknowledged. The Australian Research Council (ARC) is thanked for funding the instrumentation.

References

[1] J.W. Anthony, R.A. Bideaux, K.W. Bladh, M.C. Nichols, Handbook of Mineralogy, Mineral Data Publishing, Tuscon, Arizona, USA, 2003.
[2] L.B. Railsback, Carb. Evap. 14 (1999) 1-20.
[3] S.W.M. Blake, C. Cuff, Preparation and use of cationic halides, sequestration of carbon dioxide. (Perma-Carb Pty Ltd, Australia). Application: WO WO, 2007, p. 66pp.
[4] G.R. Hunt, R.P. Ashley, Bull. Soc.Econ.Geol. 74 (1979) 1613-1629.
[5] G.R. Hunt, R.C. Evarts, Geophysics 46 (1981) 316-321.
[6] P.P. Smolin, T.A. Ziborova, Doklady Akad. Nauk SSSR 226 (1976) 923-926
[7] G.O. Nechiporenko, G.V. Sokolova, T.A. Ziborova, G.P. Bondarenko, Min. Z. 10 (1988) 78-85.
[8] J.H. Canterford, G. Tsambourakis, B. Lambert, Min. Mag. 48 (1984) 437-442.
[9] P.J. Davies, B. Bubela, Chem.Geol. 12 (1973) 289-300.
[10] G. Raade, Am. Min. 55 (1970) 1457-1465.
[11] H.G.M. Edwards, S.E.J. Villar, J. Jehlicka, T. Munshi, Spectrochim. Act., 61A (2005) 2273-2280.
[12] E. Konigsberger, L.-C. Konigsberger, H. Gamsjager, Geochim. Cosmochim. Act. 63 (1999) 3015-3119.
[13] M. Akao, S. Iwai, Act. Crystall. B33 (1977) 3951-3953.
[14] J.R. Guenter, H.R. Oswald, J. Solid State Chem. 21 (1977) 211-215.
[15] K.N. Goswami, Indian J. Pure App. Phys. 12 (1974) 667-669.
[16] H. Jagodzinski, Mineral. Petrog. Mitt. 10 (1965) 297-330.
[17] M. deWolff, Acta Cryst. 5 (1952) 286-287.
[18] M. Fenoglio, Period. Min. 13 (1942) 1-10.
[19] L. Brugnatelli, Centr. Min. 35 (1903) 144-148.
[20] L. Brugnatelli, Rend. Ist. Lombardo 35 (1902) 869-874.
[21] R.L. Frost, J. Cejka, G.A. Ayoko, M.J. Dickfos, J. Raman Spectrosc. 39 (2008) 374-379.
[22] R.L. Frost, M.J. Dickfos, J. Cejka, J. Raman Spectrosc. 39 (2008) 582-586.
[23] R.L. Frost, M.C. Hales, D.L. Wain, J. Raman Spectrosc. 39 (2008) 108-114.
[24] R.L. Frost, E.C. Keeffe, J. Raman Spectrosc. in press (2008).
[25] S.J. Palmer, R.L. Frost, G. Ayoko, T. Nguyen, J. Raman Spectrosc. 39 (2008) 395-401.
[26] R.L. Frost, J.M. Bouzaid, J. Raman Spectrosc. 38 (2007) 873-879.
[27] R.L. Frost, J. Cejka, J. Raman Spectrosc. 38 (2007) 1488-1493.
[28] R.L. Frost, J. Cejka, M.L. Weier, W.N. Martens, G.A. Ayoko, J. Raman Spectrosc. 38 (2007) 398-409.
[29] R.L. Frost, M.L. Weier, P.A. Williams, P. Leverett, J.T. Kloprogge, J. Raman Spectrosc. 38 (2007) 574-583.
[30] W.B. White, American Mineralogist 56 (1971) 46-53.
[31] R.L. Frost, M.J. Dickfos, J. Raman Spectrosc. 38 (2007) 1516-1522.
[32] R.L. Frost, J. Raman Spectrosc. 37 (2006) 910-921.
[33] R.L. Frost, S. Bahfenne, J. Graham, B.J. Reddy, Polyhedron 27 (2008) 2069-2076.

List of Figures

Figure 12 Infrared spectra of dypingite in the 3435 to 3935 cm^{-1} region at 200, 400 and 600 °C

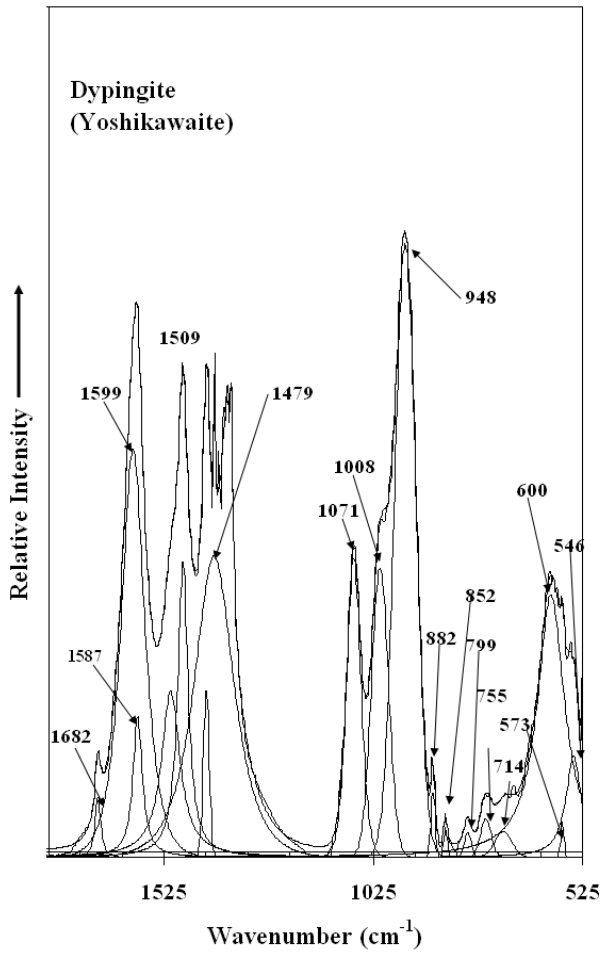
Dypingite
(Yoshikawaite)
Relative Intensity
948
1509
1599
1479
1008
1071
600
546
852
882
799
1587
755
573
1682
714
1525
1025
525
Wavenumber (cm-1)

Figure 1a

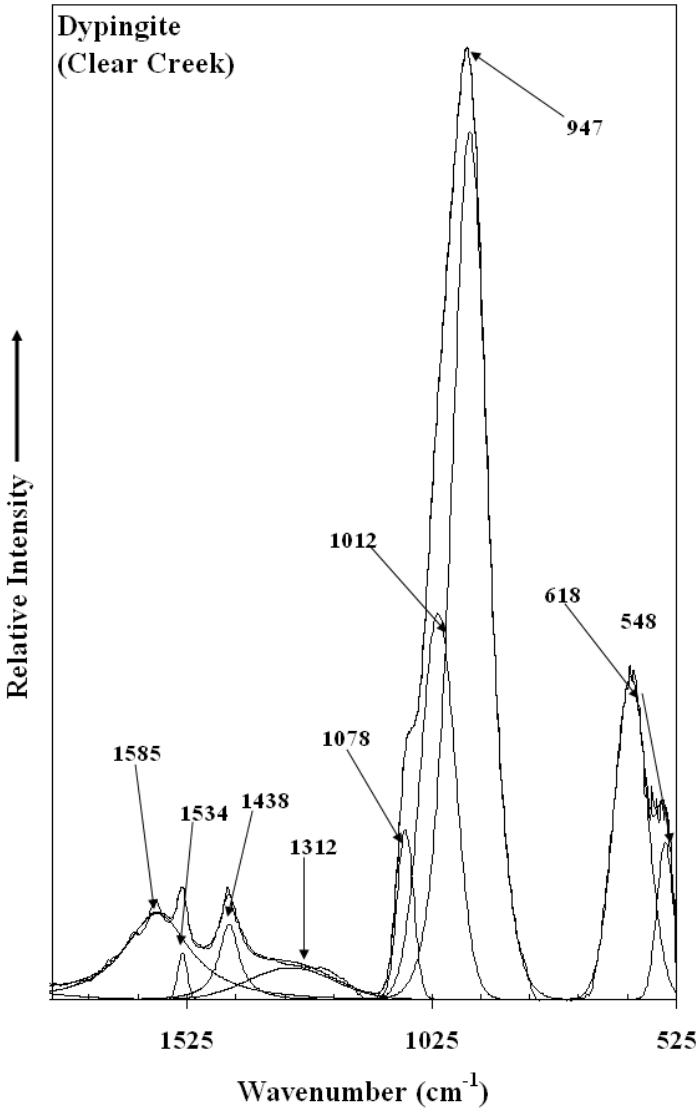
Dypingite
(Clear Creek)
947
1012
618
548
1078
1585
1534
1438
1312
Relative Intensity
1525
1025
525
Wavenumber (cm-1)

Figure 1b

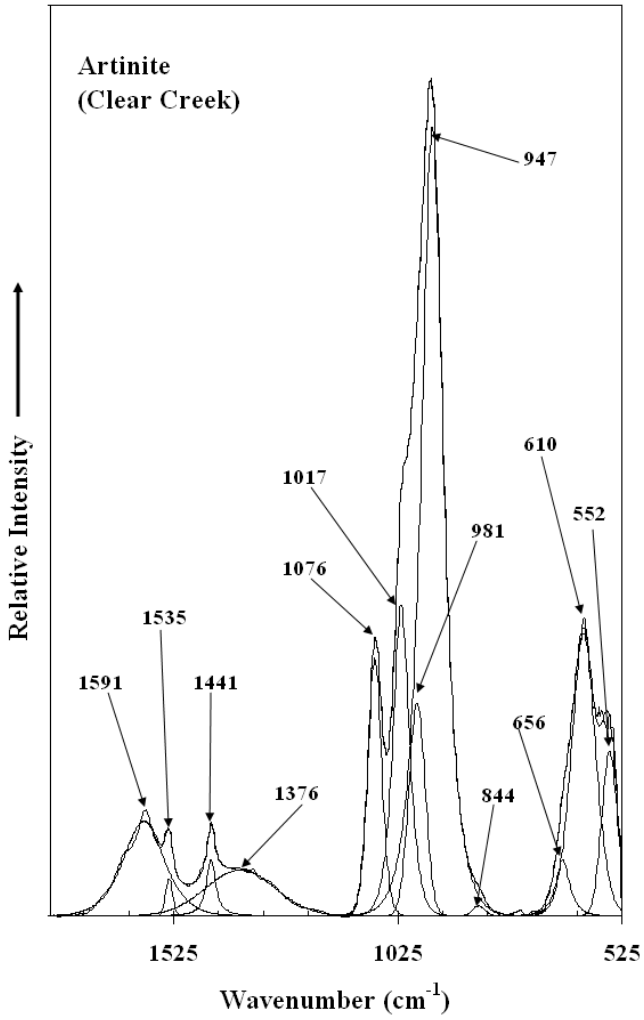
Artinite
(Clear Creek)
947
610
1017
552
981
1076
1535
1591
1441
656
1376
844
Relative Intensity
1525
1025
525
Wavenumber (cm-1)

Figure 2a

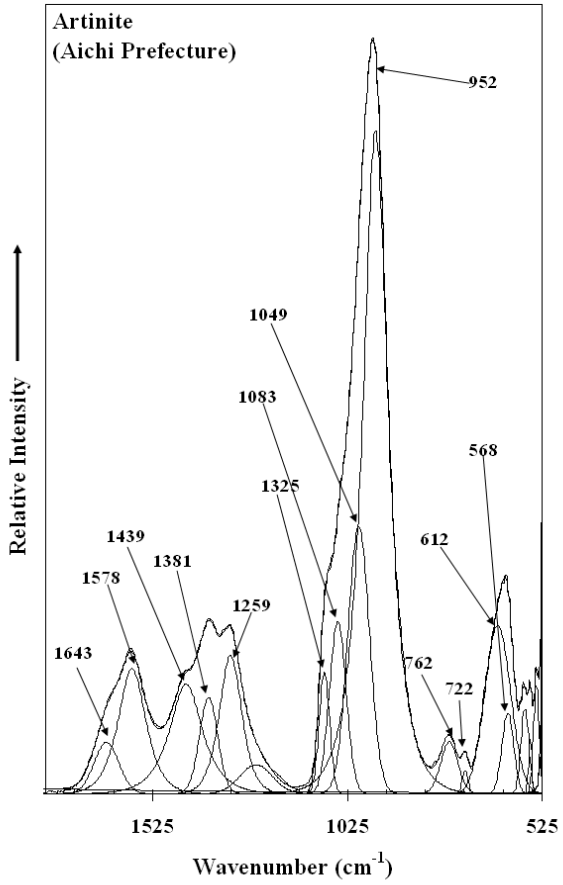
Artinite
(Aichi Prefecture)
952
1049
1083
568
1325
612
1439
1381
1578
1259
1643
762
722
Relative Intensity
1525
1025
525
Wavenumber (cm-1)

Figure 2b

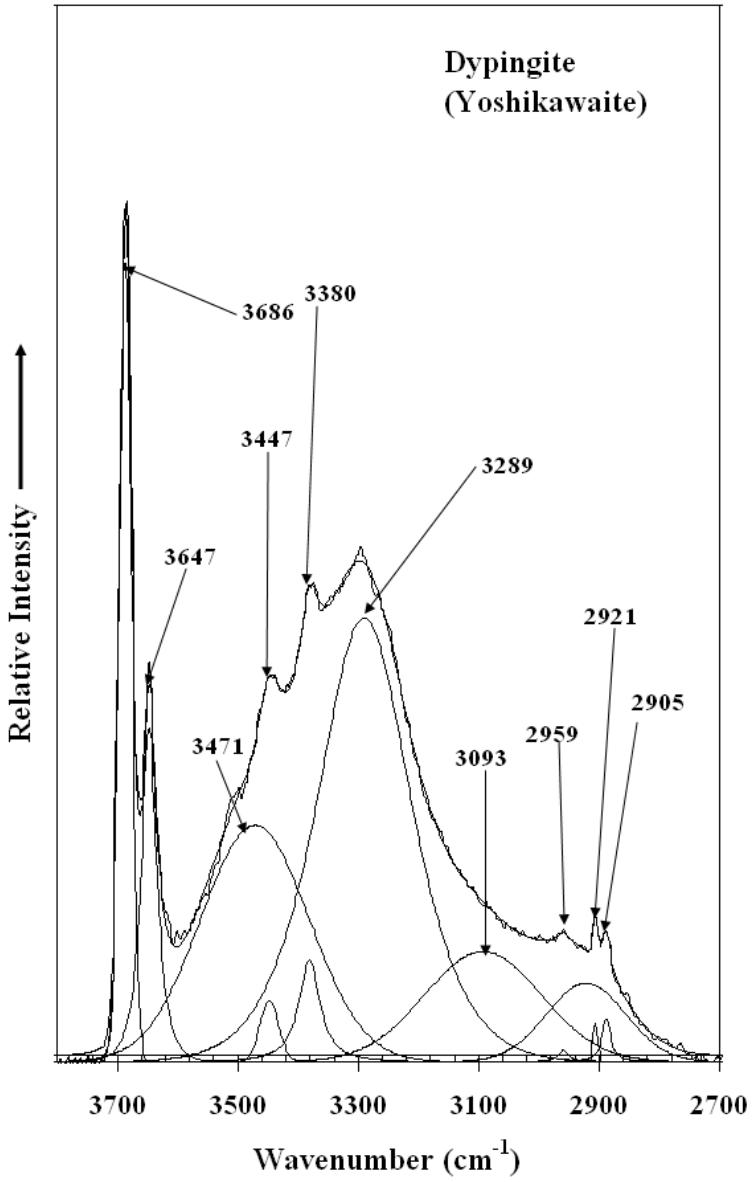
Dypingite
(Yoshikawaite)
3686
3380
3447
3289
3647
2921
2905
2959
3471
3093
Relative Intensity
3700
3500
3300
3100
2900
2700
Wavenumber (cm-1)

Figure 3a

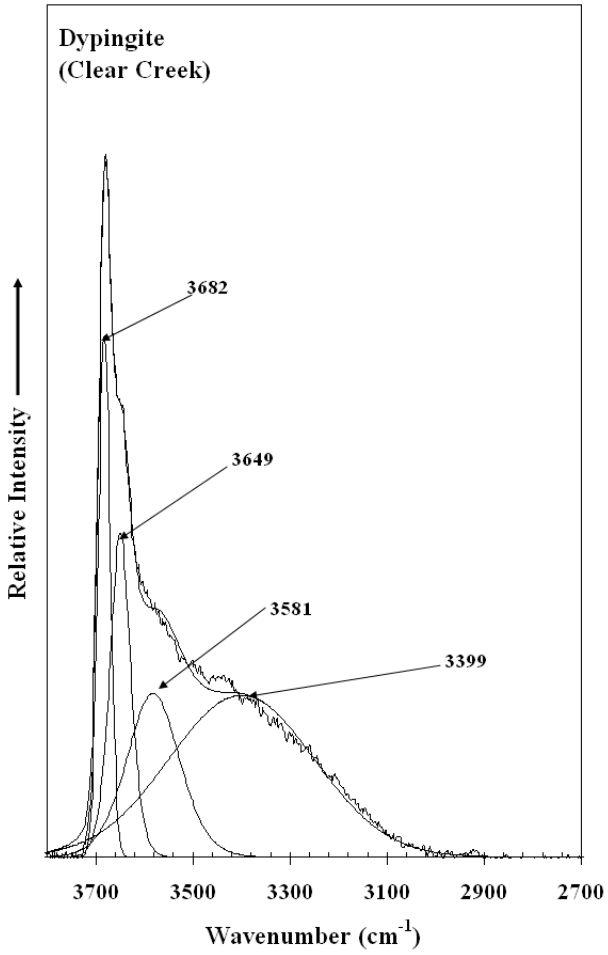
Dypingite
(Clear Creek)
3682
3649
3581
3399
Relative Intensity
3700
3500
3300
3100
2900
2700
Wavenumber (cm-1)

Figure 3b

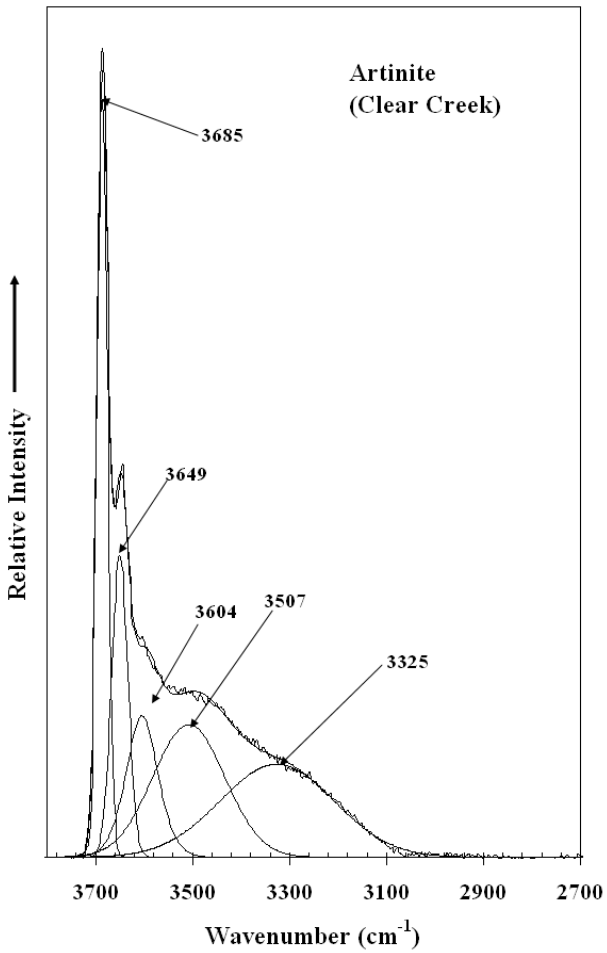
Artinite
(Clear Creek)
3685
3649
3604
3507
3325
Relative Intensity
3700
3500
3300
3100
2900
2700
Wavenumber (cm-1)

Figure 4a

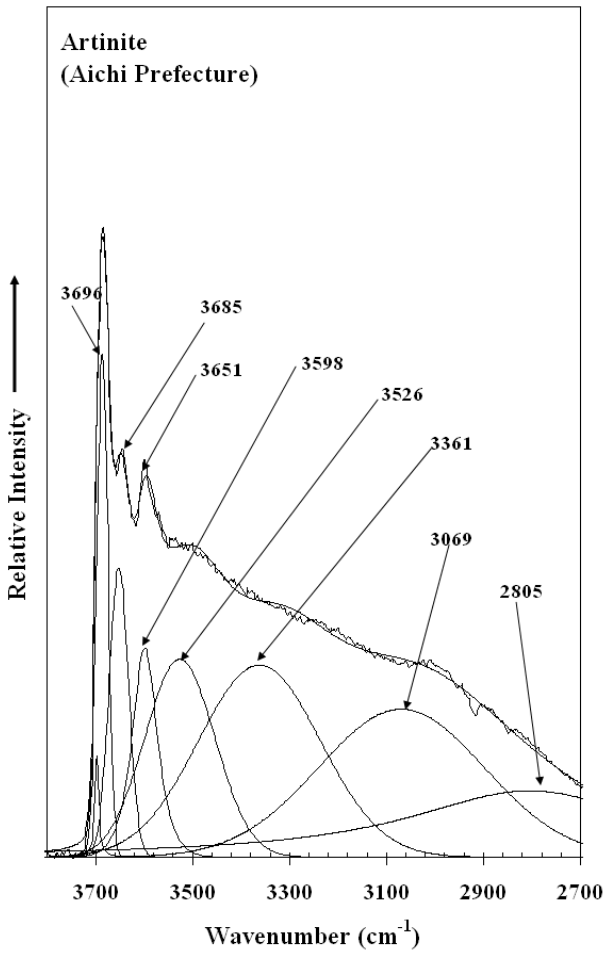
Artinite
(Aichi Prefecture)
3696
3685
3651
3598
3526
3361
3069
2805
Relative Intensity
3700
3500
3300
3100
2900
2700
Wavenumber (cm-1)

Figure 4b

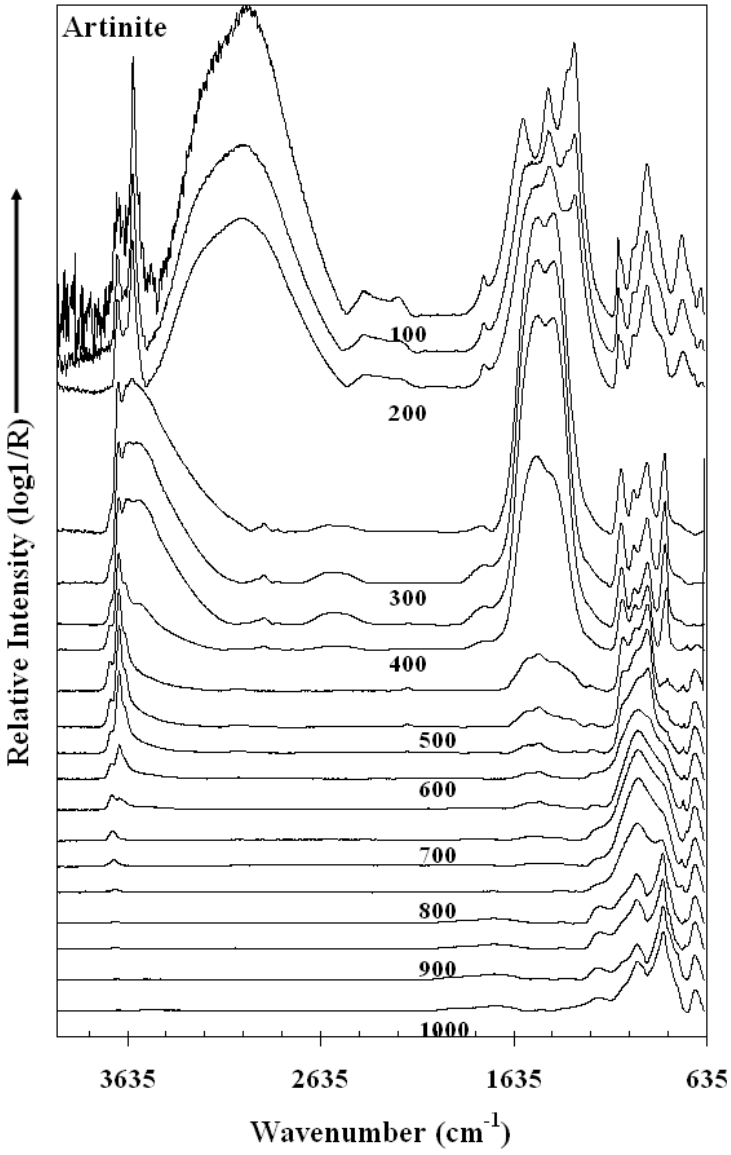

Figure 5 artinite

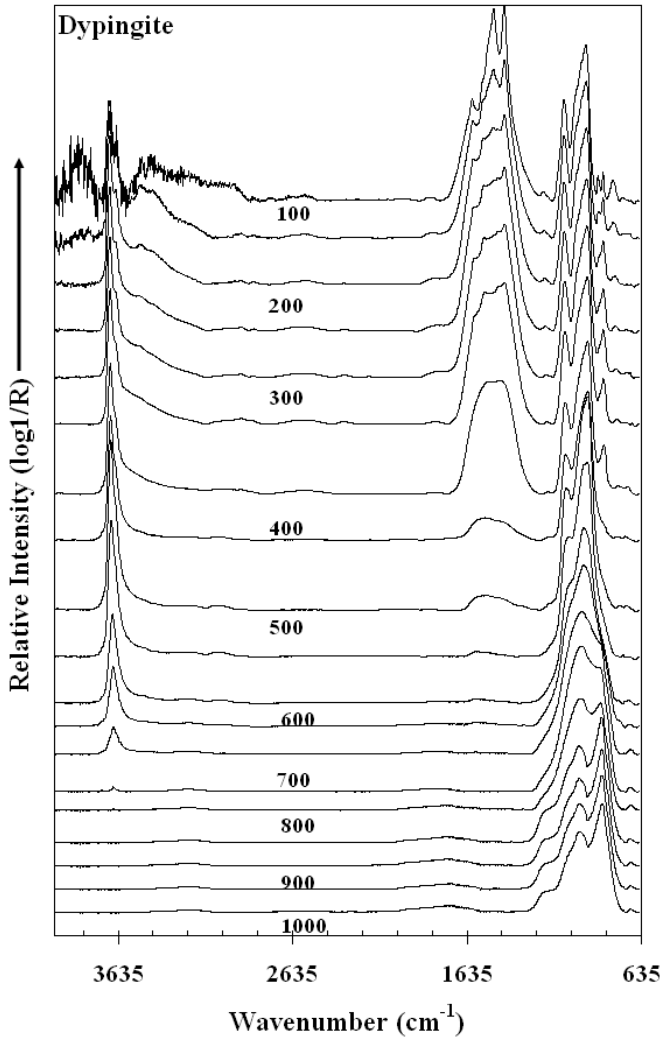
Dypingite
100
200
300
400
500
600
700
800
900
1000
Relative Intensity (log1/R)
3635
2635
1635
635
Wavenumber (cm-1)

Figure 6

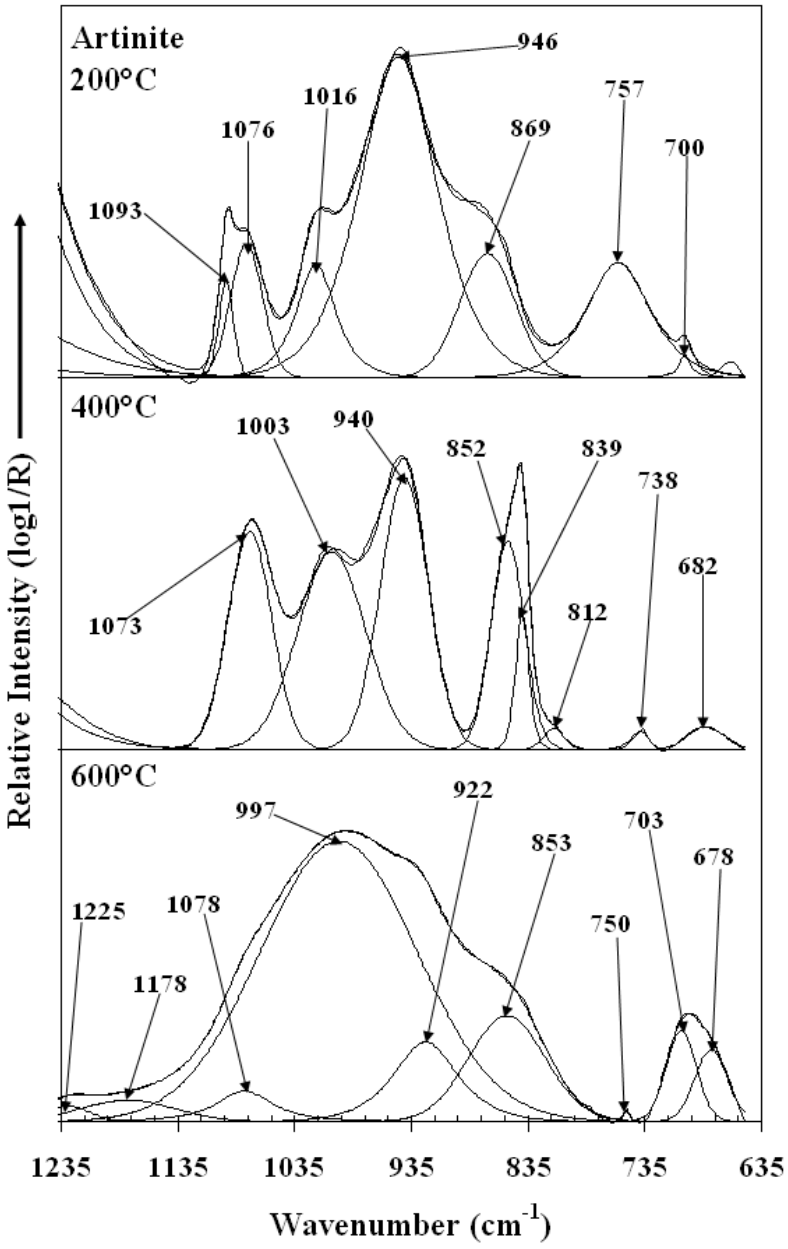
Artinite
200°C
946
1016
757
1076
869
700
1093
400°C
1003
940
852
839
738
682
1073
812
600°C
997
922
703
853
678
1225
1078
750
1178
Relative Intensity (log1/R)
1235
1135
1035
935
835
735
635
Wavenumber (cm-1)

Figure 7

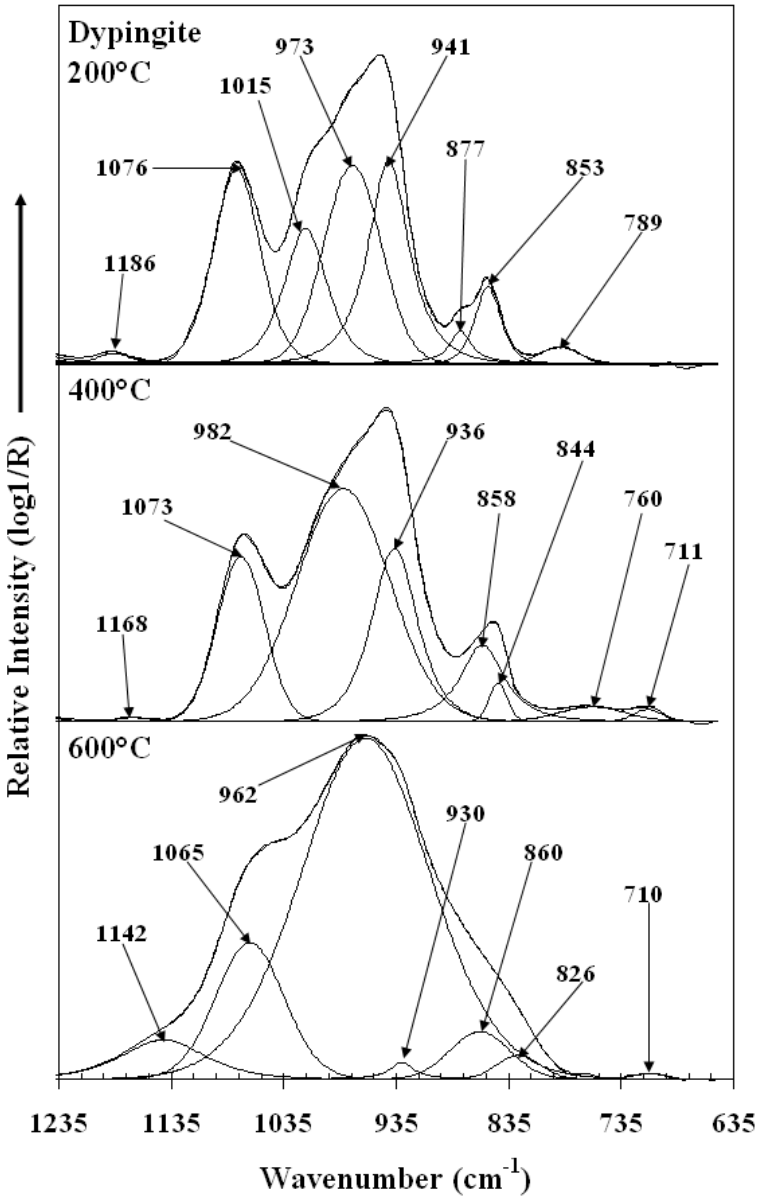
Dypingite
200°C
973
941
1015
877
1076
853
789
1186
400°C
982
936
844
1073
858
760
711
1168
600°C
962
930
1065
860
710
1142
826
Relative Intensity (log1/R)
1235
1135
1035
935
835
735
635
Wavenumber (cm-1)

Figure 8

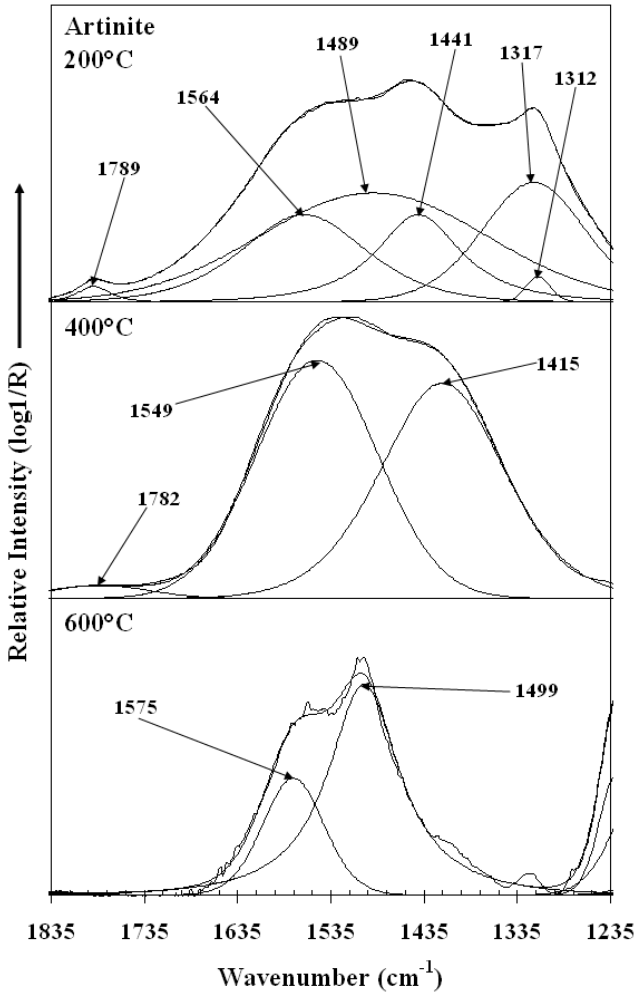
Artinite
200°C
1489
1441
1317
1312
1564
1789
400°C
1549
1415
1782
600°C
1575
1499
Relative Intensity (log1/R)
1835
1735
1635
1535
1435
1335
1235
Wavenumber (cm-1)

Figure 9

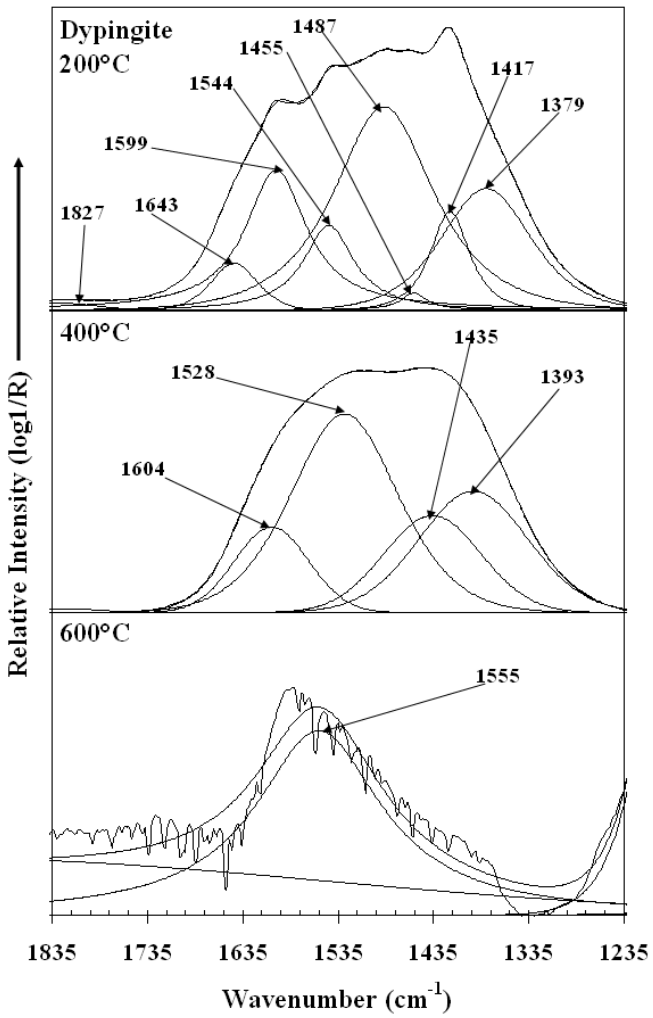
Dypingite
200°C
1487
1455
1544
1417
1379
1599
1643
1827
400°C
1435
1528
1393
1604
600°C
1555
Relative Intensity (log1/R)
1835
1735
1635
1535
1435
1335
1235
Wavenumber (cm-1)

Figure 10

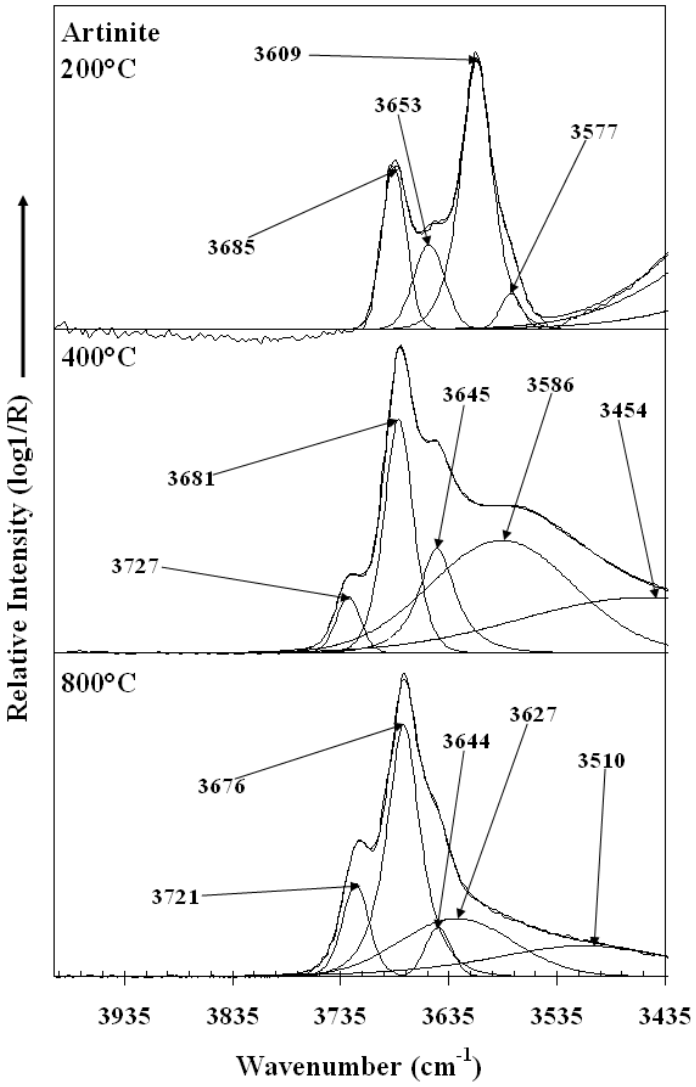
Artinite
200°C
3609
3653
3577
3685
400°C
3645
3586
3454
3681
3727
800°C
3627
3644
3510
3676
3721
Relative Intensity (log1/R)
3935
3835
3735
3635
3535
3435
Wavenumber (cm-1)

Figure 11

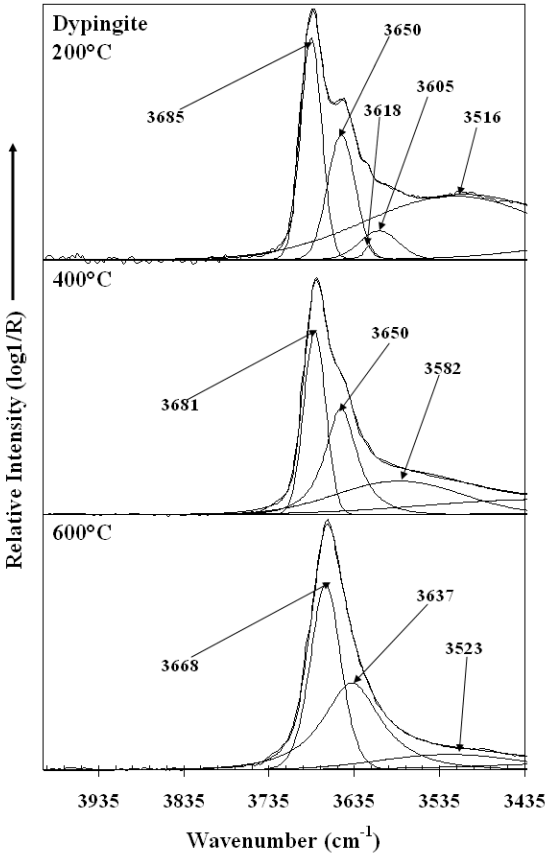
Dypingite
200°C
3685
3650
3618
3605
3516
400°C
3681
3650
3582
600°C
3668
3637
3523
Relative Intensity (log1/R)
3935
3835
3735
3635
3535
3435
Wavenumber (cm-1)

Figure 12